Molecular Microbiology (2010) 77(5), 1096–1110 ■
doi:10.1111/j.1365-2958.2010.07273.x
First published online 16 July 2010

CtpV: a putative copper exporter required for full virulence of *Mycobacterium tuberculosis*

Sarah K. Ward,[1] Bassam Abomoelak,[1] Elizabeth A. Hoye,[1] Howard Steinberg[1] and Adel M. Talaat[1,2]*

[1]*Department of Pathobiological Sciences, University of Wisconsin-Madison, 1656 Linden Drive, Madison, WI 53706, USA.*

[2]*Department of Food Hygiene, College of Veterinary Medicine, Cairo University, Giza, Egypt.*

Summary

Copper is a required micronutrient that is also toxic at excess concentrations. Currently, little is known about the role of copper in interactions between bacterial pathogens and their human hosts. In this study, we elucidate a mechanism for copper homeostasis in the human pathogen *Mycobacterium tuberculosis* via characterization of a putative copper exporter, CtpV. CtpV was shown to be required by *M. tuberculosis* to maintain resistance to copper toxicity. Furthermore, the deletion of *ctpV* resulted in a 98-gene transcriptional response, which elucidates the increased stress experienced by the bacteria in the absence of this detoxification mechanism. Interestingly, although the Δ*ctpV* mutant survives close to the wild-type levels in both murine and guinea pig models of tuberculosis, animals infected with the Δ*ctpV* mutant displayed decreased lung damage, and mutant-infected mice had a reduced immune response to the bacteria as well as a significant increase in survival time relative to mice infected with wild-type *M. tuberculosis*. Overall, our study provides the first evidence for a connection between bacterial copper response and the virulence of *M. tuberculosis*, supporting the hypothesis that copper response could be important to intracellular pathogens, in general.

Introduction

Many enzymes require a metal cofactor for activity. The metals that serve as cofactors in enzymes required for life are considered biologically active metals (biometals). These metals, including iron, copper, zinc and magnesium, are required micronutrients for many diverse cellular organisms, from humans to bacteria. For bacteria that colonize the human body, this can provide a form of environmental stress, as microbes and host cells struggle to maintain appropriate levels of the same micronutrients. The most commonly used metal cofactor, iron, has frequently been studied in the context of this struggle (Schaible and Kaufmann, 2004). Required by both host cells and bacteria for a number of enzymatic activities, including respiration and detoxification, iron is kept bound by host proteins such as transferrin and lactoferrin. Successful human pathogens, including *Mycobacterium tuberculosis* (*Mtb*), have developed iron-specific uptake mechanisms and regulators, which contribute to iron scavenging and survival within a host (De Voss *et al.*, 2000; Smith, 2003). Another biologically active metal, copper, is also required by both host and bacterial enzymes, including oxidases and superoxide dismutase (MacPherson and Murphy, 2007). The potential function of copper in host/microbe interactions has not yet been elucidated. However, studies of copper homeostasis mechanisms in pathogenic organisms have shown that copper export, in addition to acquisition, is important for virulence. For example, copper export knockout mutants of the human pathogen *Pseudomonas aeruginosa* displayed reduced colonization levels when tested in murine models, as well as the plant pathogens *Pseudomonas fluorescens* and *Xanthomonas axonopodis* when grown in plant hosts (Schwan *et al.*, 2005; Zhang and Rainey, 2007; Teixeira *et al.*, 2008).

The previous studies of biometals suggest that although pathogenic bacteria must obtain sufficient amounts of micronutrients, they are also sensitive to metal toxicity. Therefore, an equal balance of metal import and export (homeostasis) must be obtained at levels appropriate for each metal. Presumably, the ability to sense metals in the environment and regulate the expression of homeostasis mechanisms is key to maintaining intracellular metals at appropriate concentrations. Recently, the first copper-binding transcriptional regulator in *Mtb* was identified (CsoR) (Liu *et al.*, 2007), showing that this important human pathogen has the ability to respond to copper in its natural environment, the phagosome of the human macrophage. It has been shown that

Accepted 18 June, 2010. *For correspondence. E-mail atalaat@wisc.edu; Tel. (+1) 608 262 2861; Fax (+1) 608 262 7420.

copper levels in primary cultured macrophages fluctuate after phagocytosis of *Mtb*, with detected copper levels ranging from approximately 25–426 μM over a 24 h course of infection (Wagner *et al*., 2005). Additionally, it was recently shown that reactive nitrogen intermediates found in the macrophage environment cause the release of copper bound to the intracellular metallothionein protein MymT in *Mtb*, providing an indirect form of copper stress mediated by the host (Gold *et al*., 2008).

CsoR, the only known copper-binding regulator in *Mtb*, is encoded within a region of the *Mtb* genome previously associated with *in vivo* survival, named the iVEGI island (Talaat *et al*., 2004). CsoR was shown to repress the expression of its own operon, the *cso* operon, in the absence of copper (Liu *et al*., 2007). CsoR loses its ability to repress *cso* expression when it binds to copper, resulting in copper-induced *cso* gene expression occurring at levels proportional to the levels of intracellular copper. The *cso* operon includes the *ctpV* gene, which encodes a putative metal transporter previously associated with copper response in *Mtb* (Ward *et al*., 2008). In this study, we provide the first functional characterization of *ctpV*, and investigate its relevance to the development of tuberculosis. We show that CtpV is required for copper detoxification in *Mtb* and likely functions as a copper exporter. CtpV is also required for the full virulence of the bacteria in two animal models of tuberculosis, and its absence has a strong effect on host immune response to *Mtb*.

Results

Construction of mutant Mtb *strains*

Previously, the expression of the *ctpV* gene was determined to be induced by copper ions via the copper-binding transcriptional regulator CsoR (Liu *et al*., 2007). Furthermore, *ctpV* was identified as a member of the *Mtb* transcriptional response to copper at both growth-permissive and toxic physiological levels, with highest induction occurring at toxic copper levels (Ward *et al*., 2008). Sequence analysis showed that *ctpV* has strong (~70%) protein-level similarity to previously characterized copper transporters involved in copper export and import in *Escherichia coli* and *Enterococcus hirae* respectively (Ward *et al*., 2008). Due to its particularly high induction during exposure to toxic levels of copper, *ctpV* was hypothesized to encode a copper exporter required for detoxification in the presence of elevated copper.

To examine this hypothesis, a knockout mutant of *ctpV* in the virulent *Mtb* strain H37Rv was constructed (Δ*ctpV*). A 2.1 kB region of *ctpV* was replaced by a hygromycin resistance cassette using homologous recombination (Fig. 1A) (Pelicic *et al*., 1997), and the mutant was confirmed using Southern blots (Fig. 1B) as well as PCR (data not shown). Because *ctpV* is the third gene in the 4-gene *cso* operon, Δ*ctpV* was tested for possible polar effects on the downstream gene of unknown function, *rv0970*. Using reverse-transcriptase PCR, the transcription of *rv0970* in the mutant strain was confirmed (Fig. 1C). Additionally, a complemented strain was constructed by cloning the *ctpV* coding region into an integrative vector (pMV361) containing the constitutive *hsp60* promoter (Stover *et al*., 1991) and transforming this construct into the Δ*ctpV* mutant strain. Integration of *ctpV* into the Δ*ctpV* genome to construct the complemented strain Δ*ctpV*::*ctpV* was confirmed with PCR (data not shown), and restored gene expression was confirmed with qRT-PCR (Fig. S1). Notably, the expression of *ctpV* from the *hsp60* promoter in Δ*ctpV*::*ctpV* versus expression from the CsoR-regulated *cso* promoter in the wild-type strain (H37Rv) resulted in a different expression profile of *ctpV* between Δ*ctpV*::*ctpV* and H37Rv. Specifically, *ctpV* expression levels were approximately sixfold higher in Δ*ctpV*::*ctpV* relative to H37Rv in copper-free media (Fig. S1). Therefore, expression of *ctpV* in the complemented strain was not only restored, but also enhanced. Finally, a growth experiment in rich liquid media (7H9 with ADC) revealed that Δ*ctpV* and its complement Δ*ctpV*::*ctpV* had no generalized growth defects relative to H37Rv (Fig. 2A). The Δ*ctpV* mutant and the complemented strain Δ*ctpV : ctpV* were then used to experimentally characterize the role of CtpV in copper response.

CtpV is required for response to copper toxicity in Mtb

To examine the role of CtpV in copper transport, we compared copper sensitivity between Δ*ctpV* and H37Rv. Growth experiments of H37Rv, Δ*ctpV* and Δ*ctpV*::*ctpV* were measured in liquid broth cultures of minimal media (Sauton's) supplemented with defined amounts of copper, using a range of copper concentrations previously determined to be physiologically relevant (Fig. 2B) (Wagner *et al*., 2005). Comparisons of colony-forming units (cfu) between the three strains revealed that Δ*ctpV* had increased copper sensitivity relative to wild-type when grown under toxic copper conditions (500 μM $CuCl_2$). The initial inoculum (~10^6 cfu ml^{-1}) for Δ*ctpV* reached an unculturable state by 8 days, versus 14 days for H37Rv. Notably, the complemented strain displayed dramatically reduced copper toxicity and was able to withstand 500 μM copper treatment for the duration of the experiment. Presumably, this was the result of its high levels of *ctpV* expression relative to the wild-type strain prior to copper stress (Fig. S1), supporting the assertion that CtpV functions in copper export.

To further characterize *M. tuberculosis* response to copper accumulation, we measured induction of *csoR* in

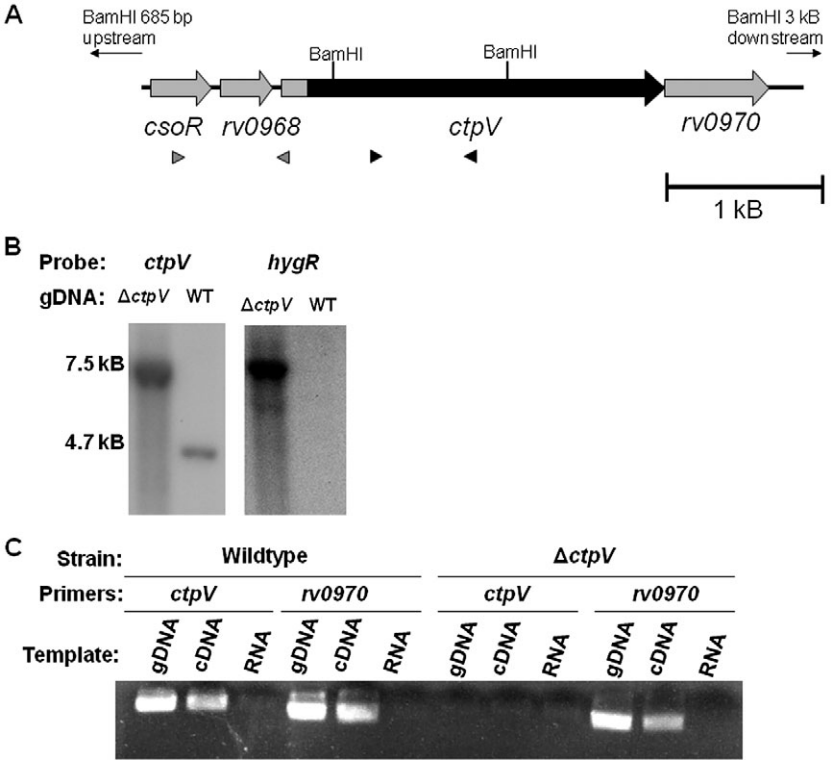

Fig. 1. Construction of Δ*ctpV* mutant using the *M. tuberculosis* H37Rv strain.
A. The Δ*ctpV* mutant was constructed with homologous recombination via pML21, a derivative of pPR27, which resulted in the deletion of 2.1 kB of the *ctpV* coding region (represented in black) and the insertion of a 3.5 kB region encoding a hygromycin resistance cassette.
B. The mutant was confirmed with Southern blots BamHI-digested genomic DNA (5 μg) from H37Rv or Δ*ctpV*. Incubation with a P32 labelled probe for the remaining *ctpV* region (left, grey arrows) revealed the increased size of the band in Δ*ctpV* (7.5 kB) relative to H37Rv (4.7 kB) resulting from the loss of two BamHI restriction enzyme sites within the *ctpV* coding region (see 1A) when it was replaced with HygR, which contains no BamHI sites. Additionally, a probe for the hygromycin resistance cassette (right, black arrows) hybridized only to the BamHI-digested gDNA from Δ*ctpV*.
C. The polarity of the *ctpV* knockout mutant was addressed using RT-PCR to check for transcription of its downstream gene. In the wild-type strain (left), positive bands show that *ctpV* and the downstream gene *rv0970* are both encoded in the genome and transcribed (able to be amplified from cDNA), with negative amplification from RNA shown as a negative control. In the isogenic mutant Δ*ctpV* (right), the *ctpV* coding region is not present in the genome or as cDNA, but transcript for the downstream gene *rv0970* is detectable.

H37Rv, Δ*ctpV* and Δ*ctpV*::*ctpV* after 3 h of exposure to 500 μM copper. Expression of *csoR* serves as a sensor of intracellular copper levels due to its autoregulation by CsoR, with increased copper leading to increased gene expression (Liu *et al.*, 2007). Results showed that *csoR* was approximately twofold upregulated in Δ*ctpV* relative to H37Rv, indicating higher intracellular copper levels (Fig. S3). Conversely, *csoR* was twofold downregulated in Δ*ctpV*::*ctpV* relative to H37Rv, indicating lower levels of intracellular copper.

CtpV deletion results in copper accumulation

Both the survival and transcriptional profiles conducted suggested the involvement of CtpV in transporting copper outside the cells. To further address this hypothesis, we directly measured copper accumulation in cells with and without CtpV using neutron activation analysis (NAA), a technique that allows for elemental quantification via the measurement of radioactive emissions following sample irradiation in a nuclear reactor (Versieck, 1994). The threshold of detection for the element Cu using NAA is relatively high, and when used NAA to measure copper levels in *M. tuberculosis*, copper quantities were too close to the detection threshold to reach statistical significance. Therefore, we used the environmental strain *Mycobacterium smegmatis* for this experiment, as it has much higher copper tolerance than *Mtb* (Fig. S4) and the bacteria could therefore be exposed to higher levels of copper prior to irradiation. Briefly, the *cso* operon was cloned into a plasmid containing an anhydrotetracycline (ATC)-inducible promoter and expression was confirmed using qRT-PCR (data not shown). *M. smegmatis* containing this plasmid (*M. smegmatis*::*cso*) as well as *M. smegmatis* containing only the empty vector (*M. smegmatis* + pSE100) were grown in copper-free media

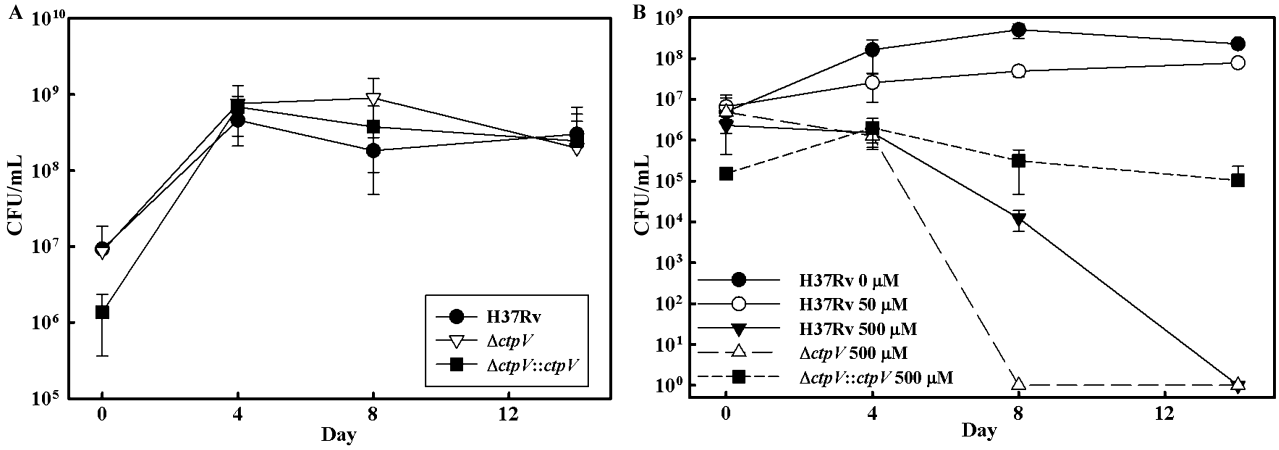

Fig. 2. Growth experiments of wild-type *Mtb* (H37Rv), Δ*ctpV* and Δ*ctpV*::*ctpV*.
A. Growth experiments of H37Rv, its isogenic mutant Δ*ctpV*, and the complemented strain Δ*ctpV : ctpV* in 7H9 + ADC liquid media. Cultures were seeded from stock to an OD_{600} of 0.10 and allowed to grow for 14 days, with cfu taken at 0, 4, 8 and 14 days via plating on 7H10 + ADC solid media. The average of two biological replicates is shown. Limit of detection = 10 cfu.
B. Cultures (30 ml) were grown in copper-free Sauton's liquid media, with defined amounts of $CuCl_2$ added. Colony-forming units (cfu) were determined at 0, 4, 8 and 14 days post exposure via plating on 7H10 + ADC solid media, plus hygromycin in the case of the mutant and complemented strains. The average of two biological replicates is shown. Growth at 0 and 50 μM was identical between the three strains, so wild-type data are shown for figure clarity (full data available in Fig. S2). Using a *t*-test, the difference between WT and Δ*ctpV* at day 8 is statistically significant ($P = 0.001$), as is the difference between WT and Δ*ctpV : ctpV* at d14 ($P = 0.02$). Limit of detection is 10 cfu. No cfu were detected for Δ*ctpV* at day 8 or for WT and Δ*ctpV* at day 14, as determined after plating 100 μl of the culture in triplicate and incubating for 6 weeks.

in the presence of ATC. Upon reaching OD 1.0, both strains were exposed to 5 mM $CuCl_2$ for 3 h, at which point the bacteria were pelleted and copper levels quantified using NAA. Results were normalized to bacterial dry mass, and revealed that the strain expressing *cso* contained significantly lower levels of copper (Fig. 3) in two

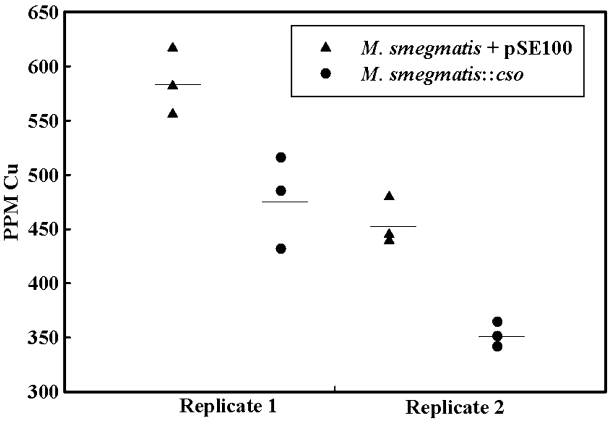

Fig. 3. Bulk analysis of copper present in cell pellets of *M. smegmatis* containing only the empty pSE100 vector as a control, or *M. smegmatis* expressing the *cso* operon, as determined by neutron activation analysis. Values are normalized to cell mass and expressed as PPM (microgram copper per gram of biomass) copper. The experiment was repeated twice and each experiment was done in triplicate. Values for *M. smegmatis* + pSE100 are significantly higher than those for *M. smegmatis*::*cso* within each replicate as determined by a T-test (replicate 1 $P = 0.02$, replicate 2 $P = 0.002$). Lines represent average value for each replicate.

independent experiments, as determined by a Student's *t*-test. The NAA experiment also tested for magnesium levels, which were not found to be different between the two strains (data not shown).

Overall, we have shown that *ctpV* is transcriptionally induced by high levels of copper (Liu *et al.*, 2007), is predicted to encode a copper transporter based on sequence analysis (Ward *et al.*, 2008), is required for resistance to copper toxicity (Fig. 2B), and that its absence results in higher levels of intracellular copper (Fig. S3 and Fig. 3). Therefore, we conclude from these experiments that CtpV is necessary for copper homeostasis in *Mtb* and likely functions as a copper exporter.

Deletion of ctpV *reveals* Mtb *stress response*

Whole-genome microarray analyses were used to investigate what transcriptional changes occur during copper stress when *ctpV* is deleted from *Mtb*. Cultures of Δ*ctpV* were exposed to 500 μM $CuCl_2$ for 3 h and transcript levels of the cells were compared with those of wild-type cultures that had been exposed to the same conditions, as published previously. This experimental set-up allowed us to identify only those genes responding to copper stress in a way unique to the Δ*ctpV* strain versus wild-type. The 3 h exposure was chosen to negate effects related to cell death that manifest after a more long-term exposure to 500 μM copper, which is known to be toxic, and was found to produce more consistent transcriptional

Table 1. Main features of copper stress response following exposure of Δ*ctpV* to toxic levels of copper, as measured by microarray analysis.

Rv name	Product	Fold change Δ*ctpV*/WT	Description
Oxidative stress			
rv1221	SigE	1.86	ECF subfamily sigma subunit
rv1909c	FurA	4.46	Ferric uptake regulatory protein
rv3146	NuoB	–1.62	NADH dehydrogenase chain B
	MymT	1.65[a]	Copper-binding metallothionein
Protein stress			
rv0055	RpsR	3.29	30S ribosomal protein S18
rv0056	RplI	1.75	50S ribosomal protein L9
rv0710	RpsQ	1.52	30S ribosomal protein S17
rv0719	RplF	–1.65	50S ribosomal protein L6
rv1298	RpmE	2.11	50S ribosomal protein L31
rv1471	TrxB	1.89	Thioredoxin reductase
rv2109c	PrcA	–2.13	Proteasome [alpha]-type subunit 1
rv3117	CysA3	–1.61	Thiosulphate sulphurtransferase
Metal substitution			
rv0247c		–1.72	Probable succinate dehydrogenase iron–sulphur subunit
rv1182	PapA3	–2.21	Polyketide synthase associated protein
rv1520		1.58	Glycosyltransferase
rv2196	QcrB	–1.82	Cytochrome b component of ubiQ-cytB reductase
rv2200c	CtaC	–1.58	Cytochrome c oxidase chain II
rv3824c	PapA1	–1.80	Polyketide synthase associated protein
rv3841	BfrB	1.75	Bacterioferritin
Membrane/exported proteins			
rv0169	Mce1A	–1.58	Cell invasion protein
rv0170	Mce1B	–1.87	Part of mce1 operon
rv0171	Mce1C	–1.59	Part of mce1 operon
rv0174	Mce1F	–1.57	Part of mce1 operon
rv1980c	Mpt64	–2.47	Secreted immunogenic protein Mpb64/Mpt64
rv2094c	TatA	3.74	TatA subunit, TAT secretion system
rv3875	EsxA	2.09	Early secretory antigen target

a. Data for *mymT* comes from qRT-PCR as the gene was not present on our arrays. The complete 98 gene data are in Table S1, and data for all *Mtb* genes are available at Array Express (http://www.ebi.ac.uk/microarray-as/ae), accession code E-MEXP-2773.

changes relative to 15 min and 24 h exposure times. Using a Nimblegen-based microarray protocol, 98 genes with significantly different expression levels between Δ*ctpV* and H37Rv after exposure to 500 μM $CuCl_2$ were identified (Table S1). To confirm the validity of the microarray data, expression levels of nine of the genes identified in the microarray dataset were tested with qRT-PCR. The changes in gene transcript levels detected by microarray were similar to that determined by qRT-PCR for all nine genes (Fig. S5).

The 98 genes identified are indicative of copper toxicity (examples in Table 1), which is thought to be the result of many combined effects that high copper levels have on cellular components. We summarized these effects in the following four categories. First, the redox capacity of copper, which can exist in either a Cu^{1+} or Cu^{2+} state, causes oxidative stress via the creation of reactive oxygen species within the cell (Pinto *et al.*, 2003). The deletion of *ctpV* affected transcription of genes previously associated with oxidative stress, such as the regulator-encoding genes *furA* and *sigE*, as well as *nuoB*, predicted to encode an NADH dehydrogenase. In total, 14 of the 98 genes identified have been previously associated with oxidative stress in *Mtb* (Schnappinger *et al.*, 2003). We also used qRT-PCR to test expression of a recently discovered gene associated with copper stress response, encoding the copper-chelating protein MymT (Gold *et al.*, 2008), that was not present on the microarray slides, and found it to be significantly upregulated in Δ*ctpV.*

Second, copper stress causes protein denaturation, particularly via interactions between copper and thiol groups (Agarwal *et al.*, 1989). A number of genes associated with protein synthesis and protein destruction were identified, including five genes predicted to encode ribosomal proteins (*rpsR, rplI, rpsQ, rplF* and *rpmE*), proteasome subunit-encoding *prcA* and genes encoding enzymes such as thiosulphate sulphurtransferase (*cysA3*) and thioredoxin reducatse (*trxB*).

Third, copper can inappropriately bind to enzymes that require other biometals for activity, resulting in enzyme inactivation (Meharg, 1994; Macomber and Imlay, 2009). Examples of this group include genes for metalloenzymes such as Mg^{2+}-requiring glycosyltransferase (*rv1520*) and polyketide synthases (*papA1, papA3*), along with components of the copper-requiring cytochrome c oxidase system (*qcrB, ctaC*). Additionally, genes associated with iron homeostasis and acquisition were also identified, including upregulation of *bfrB*,

encoding a bacterioferritin, and downregulation of *rv0247c*, encoding an iron–sulphur protein, which is consistent with previously identified connections between copper homeostasis and iron (Chung *et al.*, 2004; Kershaw *et al.*, 2005; Teitzel *et al.*, 2006).

Fourth, copper causes membrane stress and destabilization (Ohsumi *et al.*, 1988; Avery *et al.*, 1996), and the largest functional group identified ($n = 16$ genes) was that of genes predicted to encode membrane and secreted proteins (Table S1). This includes several *mce* genes (*mce1A, mce1B, mce1C, mce1F*) as well as *tatA*, encoding a component of the Tat secretion system thought to be responsible for transport of the copper detoxification enzyme multi-copper oxidase (Graubner *et al.*, 2007) as well as the antigenic proteins Ag85A and Ag85C (Marrichi *et al.*, 2008). Genes for secreted proteins such as *mpt64* and *esxA* were also identified.

Because copper exposure has been shown to cause membrane instability and visible morphological changes (Ohsumi *et al.*, 1988), we performed scanning electron microscopy analysis of the Δ*ctpV* and H37Rv strains under copper-free or high-copper conditions (Fig. S6). Results confirmed that there was no gross morphological difference between the two strains, and also demonstrated that copper stress did not have a visible effect on membrane shape or size in either strain. Despite the lack of a visible difference in cell wall stability, the microarray data points to an effect of the *ctpV* deletion, and presumably increased intracellular copper, on the membrane and exported protein profile of Δ*ctpV.* Notably, many of the secreted proteins identified are predicted to be immunogenic. Overall, the *Mtb* genes identified in this study fit into four categories associated with the effects of copper stress, suggesting that the Δ*ctpV* bacteria experienced increased copper stress relative to wild-type when exposed to the same level of copper.

Redundancy of CtpV

Interestingly, the genome of *Mtb* encodes a number of genes with high sequence similarity to *ctpV*. Specifically, *ctpV* is classified as encoding a metal translocation P-type ATPase protein, and there are 10 other predicted metal-translocation P-type ATPases in the H37Rv genome with significant sequence similarity to *ctpV* (Table S2), representing possible functional redundancy for copper export within the *Mtb* genome.

To precisely investigate whether any of the other P-type ATPases encoded by *Mtb* might be upregulated in the absence of *ctpV*, qRT-PCR was used to measure the transcriptional induction of the panel of 11 ATPases present in the *Mtb* genome. These data revealed that only one other gene encoding a P-type ATPase, *ctpG*, is

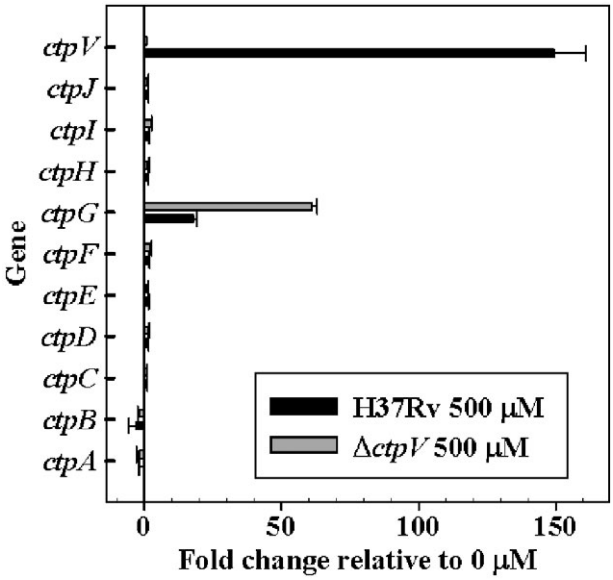

Fig. 4. Transcriptional responses to the deletion of *ctpV* under toxic levels of copper. Transcript levels of all genes within the *Mtb* genome predicated to encode metal-transporting P-type ATPases at 500 μM versus 0 μM copper, in both H37Rv and Δ*ctpV*, were measured using qRT-PCR. Data are displayed as fold-change relative to expression at 0 μM Cu, and are normalized to expression of 16S rRNA. Averaged data from two biological replicates are shown.

induced in the presence of copper (20-fold), and furthermore, that it is particularly induced (60-fold) in the absence of *ctpV* (Fig. 4). Notably, expression levels of the *ctpA* and *ctpB* genes were unchanged, despite the presence of copper transport-associated motifs in their protein sequences. The predicted protein sequence of *ctpG* contains motifs common to P-type ATPase transporters in general, but lacks the motif associated with copper-specific transporters (Fig. S7), and has been predicted via sequence analysis to belong to a family of Cd, Pb, Zn and Co transporters (http://traplabs.dk/patbase/). It has also been shown to be regulated by CmtR, an SmtB-ArsR family cadmium- and lead-responsive repressor (Wang *et al.*, 2005) that was identified via microarrays as responsive to general copper stress as well as the absence of *ctpV* (this study). Additionally, the lack of copper-induced transcriptional induction of the other predicted transporter-encoding genes, including *ctpA* and *ctpB*, does not exclude the possibility that they could function as copper exporters, which may be constitutively expressed or regulated in a copper-independent manner. Overall, the high number of predicted metal transporters suggests the evolutionary value of metal response in *Mtb*, and it seems likely that other encoded genes are functionally redundant with *ctpV*. Genomic and transcriptional data point to *ctpA, ctpB* and *ctpG* as possible targets of future investigation.

CtpV is required for full virulence in guinea pigs

The *ctpV* gene is part of a 29-gene genomic island previously shown to be preferentially induced in mice relative to *in vitro* culture (termed the *in vivo* expressed genomic island, iVEGI) (Talaat *et al*., 2004). This suggested that *ctpV* might play a role specific to the *in vivo* lifestyle of *Mtb*. In addition, our experiments showed that CtpV is necessary to maintain copper homeostasis, and data from other groups suggest that copper homeostasis in bacteria may play a role in pathogenesis (Francis and Thomas, 1997; Mitrakul *et al*., 2004; Schwan *et al*., 2005), although this had never been tested in *Mtb*. To investigate the role of *ctpV* in a host infection model, groups of guinea pigs ($n = 12$) were infected with H37Rv, Δ*ctpV* or Δ*ctpV*::*ctpV* via an aerosol infection route. Colony-forming units within lung tissue were determined at 1, 21 and 42 days post infection, and lung tissues were sectioned and stained for histopathological examination. Colony counts for the Δ*ctpV* mutant were significantly lower than those of H37Rv at 21 days post infection ($P = 0.04$) (Fig. 5A). However, by 42 days post infection no colonization defect remained.

The histology staining of infected guinea pig tissue revealed that the tissue damage seen in the guinea pigs infected with H37Rv or Δ*ctpV*::*ctpV* was more extensive than the tissue damage seen in the guinea pigs infected with Δ*ctpV.* Specifically, larger portions of lung lobes were damaged in the H37Rv-infected guinea pigs compared with those infected with Δ*ctpV*, especially at 42 days post infection (Fig. 5B). Additionally, granulomatous responses were more severe in lungs collected from H37Rv or Δ*ctpV*::*ctpV* -infected animals compared with those infected with Δ*ctpV* (Fig. 5B). Both the colonization and pathological data in guinea pigs suggested a role played by *ctpV* in full virulence of *Mtb*. To further investigate the role of CtpV in virulence, we continued our study of pathogenesis within the murine model of tuberculosis.

CtpV is required for full virulence of Mtb *in a murine model*

Groups of BALB/c mice ($n = 30$–40) were infected with H37Rv, Δ*ctpV* or Δ*ctpV*::*ctpV* using a low-dose aerosolization protocol. Bacterial colony counts from mouse lung tissue over the course of the infection revealed that bacterial survival between the three strains over the course of infection was similar, and differences in colonization levels did not reach statistical significance at any time point (Fig. 6A). Nonetheless, mice infected with Δ*ctpV* lived significantly longer than mice infected with wild-type, with 16-week increase in time-to-death versus mice infected with H37Rv (Fig. 6B). In fact, the median survival time for mice infected with H37Rv was 31 weeks, versus 47 weeks for mice infected with Δ*ctpV* and 42 weeks for mice infected with Δ*ctpV*::*ctpV.* As determined by a log-rank statistical test (Petrie and Watson, 2006), survival was significantly different between the H37Rv and Δ*ctpV* infection (P-value = 0.002), although survival was also significantly different between the H37Rv and Δ*ctpV*::*ctpV* infection (P-value = 0.02).

Despite carrying similar bacterial loads throughout the infection, histology of the infected mouse tissue revealed consistently lower levels of tissue damage in mice infected with Δ*ctpV* versus the wild-type and complemented strains. For example, at 8 weeks post infection, lung tissue from mice infected with Δ*ctpV* displayed granulomatous inflammation, whereas mice infected with H37Rv displayed massive granulomatous inflammation with more lymphocytic infiltration (Fig. 7A). By 38 weeks post infection, granulomas became more developed (presence of giant cells) and occupied almost the whole lungs of mice infected with H37Rv, compared with only 50% of tissues of mice infected with the Δ*ctpV* mutant (Fig. 7B). Lesions observed in the complemented strain were very similar to those observed in mice infected with H37Rv strain. Overall, mouse survival and histopathological data indicated the attenuation of the Δ*ctpV* mutant compared with other tested strains.

Immune response to infection is altered by CtpV deletion

Lung pathology in tuberculosis is thought to be caused mainly by the host immune response (Rook *et al*., 1991). Therefore, to investigate a possible mechanism for the decreased lung pathology of animals infected with Δ*ctpV* relative to H37Rv and Δ*ctpV*:: *ctpV*, lung sections from the murine infection were stained with an antibody against mouse interferon-γ (IFN-γ), a key cytokine known to be highly expressed during tuberculosis infection (Flynn and Chan, 2001). As expected, no indication of IFN-γ expression was seen at 2 weeks post infection, prior to the start of the adaptive immune response (data not shown). However, by 8 weeks post infection, mice infected with H37Rv show significant IFN-γ expression, localized in areas of lung tissue damage, yet mice infected with Δ*ctpV* showed only small amounts of IFN-γ expression (Fig. 7C). Mice infected with Δ*ctpV*::*ctpV* showed an intermediate level of IFN-γ expression. Interestingly, even at the 38-week time point where mice infected with Δ*ctpV* display large amounts of tissue damage, there was still little expression of IFN-γ relative to mice infected with H37Rv (Fig. 7D). Overall, our analysis indicates contributions of copper response genes to triggering the host immune responses.

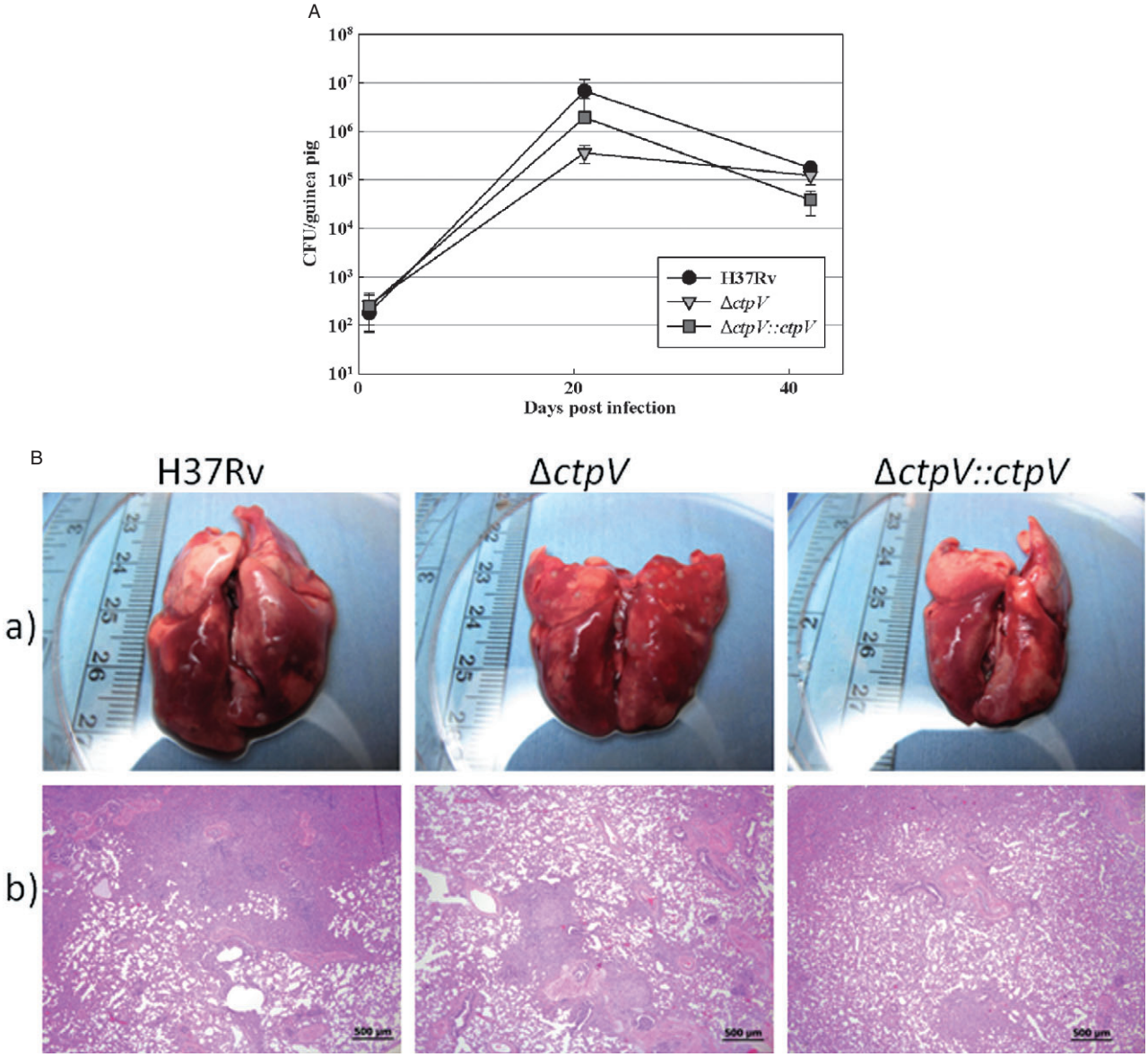

Fig. 5. Guinea pigs infection with *M. tuberculosis* and its isogenic mutant Δ*ctpV*.
A. Bacterial colonization of guinea pig lungs after aerosol infection with either wild-type H37Rv, Δ*ctpV* or the complemented strain Δ*ctpV*::*ctpV*. Colony-forming units were determined following homogenization of lungs from infected guinea pigs. Colonization levels between H37Rv and Δ*ctpV* are statistically different at 21 days post infection ($P = 0.04$) but not at 42 days post infection. The experiment was performed once with 3–4 animals per strain per time point.
B. Pathology of infected guinea pigs. (a) Necropsy of lungs of guinea pigs infected with the H37Rv, Δ*ctpV*, and Δ*ctpV*::*ctpV* at 42 days post infection. (b) Haematoxylin and eosin (H&E) stained guinea pig tissue (40 × magnification, scale bar = 500 μm) at 42 days post infection are shown.

Discussion

Tuberculosis kills approximately 1.6 million people per year, making *Mycobacterium tuberculosis* the most deadly bacterial pathogen worldwide (Lopez *et al*., 2006). Understanding the response of *Mtb* to its intracellular environment, as well as the host response to *Mtb* infection, is key to learning to combat this global threat. Interplay of hosts and pathogens in response to biometals is known to play a role in bacterial infections. However, metal ion homeostasis in *Mtb*, as in most pathogens, has previously been studied mainly in the context of iron deprivation. On the other hand, the role of copper in bacterial infections has not yet been clearly defined. Several studies, including this one, have begun to elucidate a connection between copper response and bacterial pathogenesis. Bacterial infections in humans have long been shown to correlate with increased copper levels in the blood (Beisel *et al*., 1974;

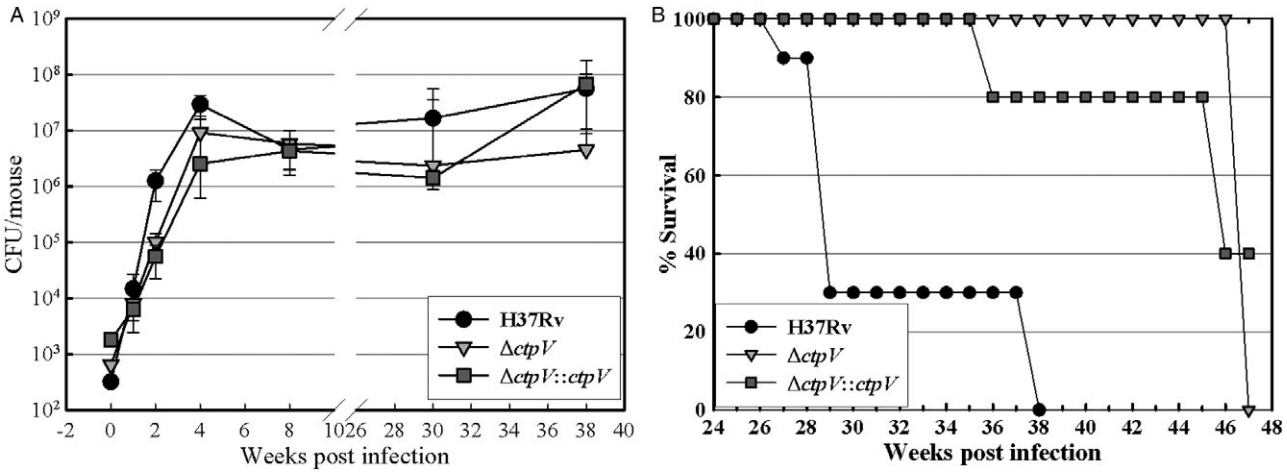

Fig. 6. Murine infection with Δ*ctpV*.
A. Bacterial colonization of mouse lungs after aerosol infection with either wild-type H37Rv, its isogenic mutant Δ*ctpV*, or the complemented strain Δ*ctpV*::*ctpV*. Colony-forming units were determined via homogenization of lungs from infected mice (N = 3–5 per time point) in PBS and plating on 7H10 + ADC, with hygromycin added in the case of the mutant and complemented strain. Colonization levels between the three strains did not display a statistically significant difference over the course of the infection. The experiment was performed twice for early time points and once for late time points.
B. Survival of mouse groups after aerosol infection with H37Rv, Δ*ctpV* or Δ*ctpV*::*ctpV*. Survival is displayed as the time from infection (week 0) until the time declared morbid by animal care staff. Morbid mice were subsequently euthanized, with tuberculosis determined as the cause of illness via necropsy. A log-rank statistical test was used to analyse survival of mice groups. Survival of mice infected with H37Rv was significantly different from those infection with Δ*ctpV* (*P*-value = 0.002), and those infected with the Δ*ctpV*::*ctpV* strain (*P*-value = 0.02). Experiment was performed once with 5–10 mice/group.

Fleming *et al*., 1991), and availability of copper ions has previously been correlated with antibacterial abilities of macrophages (Percival, 1998). Copper levels in the phagosome fluctuate via unknown mechanisms after phagocytosis of mycobacteria, as well as after stimulation with IFN-γ (Wagner *et al*., 2005). Interestingly, hypoxia, a condition found in mycobacterial granulomas, has recently been shown to trigger copper uptake in macrophages through upregulation of the macrophage copper transporter CTR1 (White *et al*., 2009). In addition, macrophage production of reactive nitrogen intermediates, known to be a major stressor in mycobacterial phagosomes, has been shown to stimulate the release of copper from mycobacterial metallothioneins (Gold *et al*., 2008). Together, these data suggest that copper toxicity is a form of stress experienced by *Mtb* and other pathogens that reside within the human macrophage.

So far, little is known about the mechanisms used by *Mtb* to resist copper toxicity. Experiments reported here suggest that *ctpV* is involved in the copper efflux response of *Mtb* to copper stress. Animal infection studies further suggest a relationship between copper response and host immunity and pathogenicity of the bacteria. Further, genomic studies show that *ctpV* is likely only one component of a larger arsenal of genes involved in copper efflux and detoxification. Interestingly, despite the large number of metal-efflux related genes encoded within the *Mtb* genome, *Mtb* is actually much more sensitive to copper than environmental strains such as *M. smegmatis*. The intracellular concentration of copper is kept so low that even sensitive techniques such as ICP-MS and NAA did not yield consistent copper measurements, requiring the use of a heterologous host for direct copper quantification. We are pursuing the use of a highly sensitive electron-microscopy based technique to measure individual copper atoms within *Mtb*.

In other pathogenic bacteria such as *P. aeruginosa* and *L. monocytogenes*, reduction of copper transport ability has been shown to cause decreased colonization levels within a host model system (Francis and Thomas, 1997; Schwan *et al*., 2005). However, in *Mtb* the deletion of *ctpV* did not lead to a significant drop in colonization levels in a murine model, but rather to an effect on lung pathology of the host. Decreased lung damage was observed in both mice and guinea pigs infected with Δ*ctpV* throughout the course of the infection. Lung damage in tuberculosis infections is hypothesized to be mainly the result of the host immune response, and in our murine experiments this decreased lung pathology correlated with decreased IFN-γ production. IFN-γ expression is associated with a protective response to *Mtb* in both mice and humans via activation of macrophages (Flynn and Chan, 2001; Casanova and Abel, 2002). Its expression by Th1 cells in response to IL-12 stimulation by macrophages is considered a key aspect of the adaptive immune response to *Mtb*. It is unclear therefore whether the decrease in host INF-γ expression is due to a decrease in IFN-γ production by Th1 cells, possibly via an effect of *Mtb* on IL-12

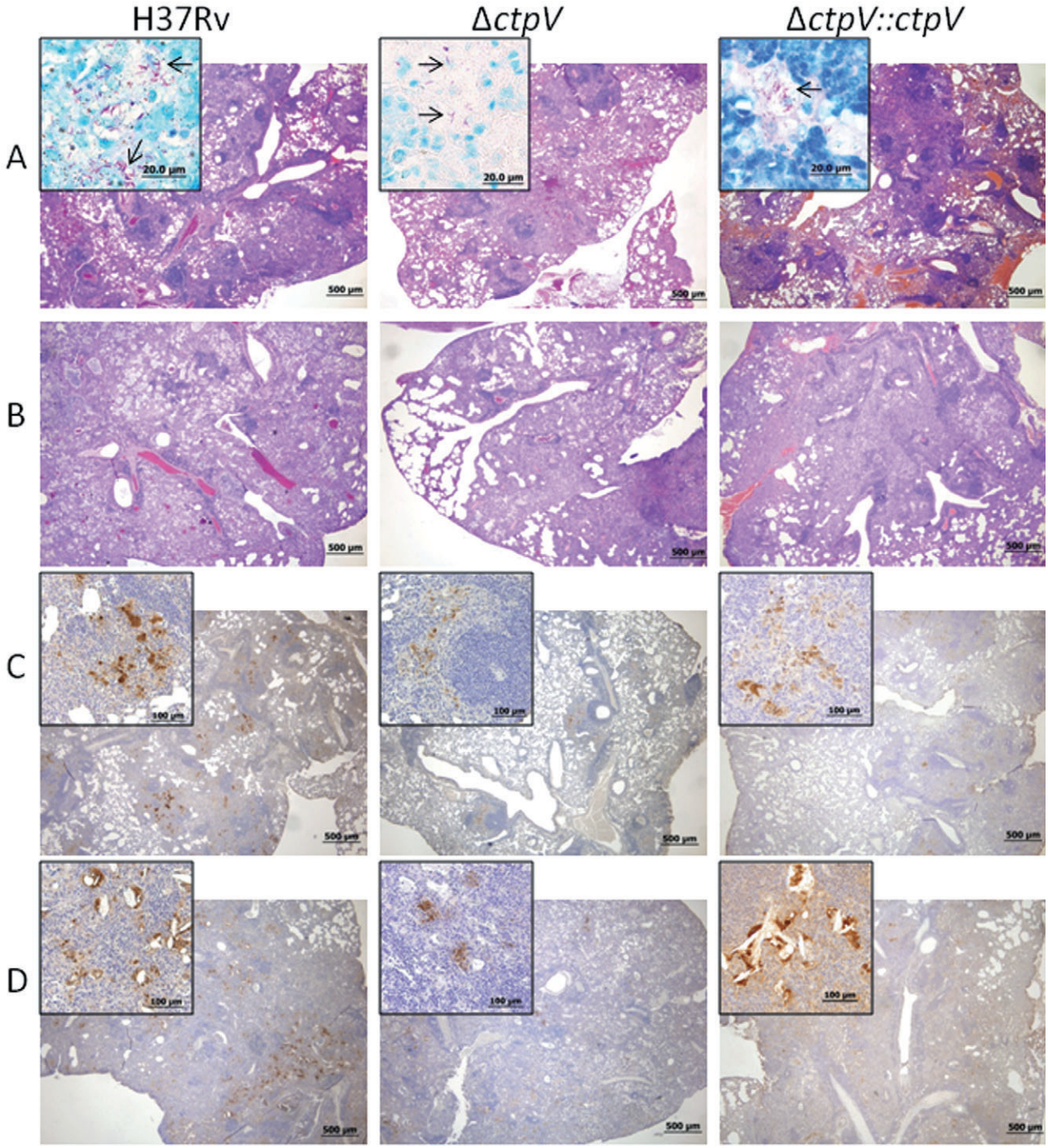

Fig. 7. Pathology of murine infection with H37Rv, Δ*ctpV* and Δ*ctpV*::*ctpV.*
A. H&E stained mouse lung tissue (40 × magnification, scale bar = 500 µm) at 8 weeks post infection. Inset images (1000 × magnification, scale bar = 20 µm) show the *Mtb* bacilli (purple), which were visible in lung tissue starting from 8 weeks forward.
B. H&E stained mouse lung tissue (40 × magnification) at 38 weeks post infection.
C. Immunohistochemisty of infected murine lung tissue at 8 weeks post infection. Murine lung tissue was sectioned and stained with antibody for mouse IFN-γ, which appears brown in the images (40 × magnification). Inset images (200 × magnification) of lesions displaying IFN-γ expression.
D. Immunohistochemisty of infected murine lung tissue at 38 weeks post infection. Inset images (200 × magnification) of lesions displaying IFN-γ expression.

secretion, or whether the apparent decrease is in fact caused by reduced migration of Th1 cells to the site of infection due to unknown immunomodulatory activities of the CtpV-deficient bacteria.

Unexpectedly, the Δ*ctpV* bacteria did not grow to higher levels or at a faster rate than the wild-type bacteria in mouse lungs, despite the lower levels of IFN-γ, which is known to be protective against *Mtb* infection. It is possible that the Δ*ctpV* bacteria succumb more easily to other *in vivo* stimuli (e.g. copper in the phagosome), resulting in apparently similar growth rates with H37Rv. Therefore, Δ*ctpV* might in fact share the colonization defect seen in other pathogens, but the decreased immune response obscures the ability to detect the attenuation. Alternatively, a decrease in IFN-γ production could be compensated for if other mechanisms of macrophage activation are upregulated, resulting in similar rates of bacterial growth with different rates of host tissue damage. Analysing the full array of cytokines produced during Δ*ctpV* or H37Rv infection, including IL-12 and TNF-α, the cytokine thought to be largely responsible for host tissue damage, will help elucidate the reason for the differences in pathology.

The basis for the different host response to Δ*ctpV* has yet to be determined. It is possible that the Δ*ctpV* strain doesn't express, or expresses at altered levels, proteins that are normally immunomodulatory. This could result either from immunogenicity of CtpV itself, and/or it could stem from the difference in expression profiles between the two strains, including altered levels of secreted proteins known to be immunogenic. For example, a large number of genes ($n = 98$) were affected by disruption of *ctpV* following exposure to toxic levels of copper. In addition, the host response could be affected by the levels of copper in the phagosome. Because mycobacterial intracellular copper concentration is higher in Δ*ctpV*, it is possible that extracellular (phagosomal) levels of copper are lower, which could affect overall immune response. Overall, our data combined with that of previous studies suggest that copper homeostasis mechanisms may play a role in the outcome of bacterial infections, but the exact role for copper ions as an antibacterial response mechanism and/or immunomodulatory molecule has yet to be determined and warrants further investigation.

Experimental procedures

Mtb *strains and mutant construction*

Experiments were performed with *Mtb* strain H37Rv, its isogenic mutant Δ*ctpV* or the complemented strain Δ*ctpV*::*ctpV*. To construct Δ*ctpV*, 800 basepair fragments of both the upstream and downstream portion of the gene were amplified by PCR (primers listed in Table S3) and cloned into the pGEM-T Easy vector (Promega, Madison, WI). The fragments were digested with their flanking restriction enzyme sites (AflII/XbaI and HindIII/SpeI for upstream and downstream portions respectively) and ligated into pYUB854 (Bardarov *et al*., 2002). After digestion by NotI and SpeI (Promega), the linearized vector was ligated into pML19, a derivative of pPR27 (Pelicic *et al*., 1997) where a kanamycin resistance cassette has been inserted into the PstI site. The resulting vector was named pML21. This vector was electroporated into electrocompetent *Mtb* using a Gene Pulser II machine (Bio-Rad, Hercules, CA, USA), and cells were plated onto Middlebrook 7H10 supplemented with 10% albumin-dextrose-catalase (ADC) and 50 μg ml^{-1} hygromycin (Invitrogen, Carlsbad, CA, USA). After one month of growth at 32°C, transformants were grown for 2 weeks with shaking 32°C in Middlebrook 7H9 supplemented with 10% ADC and 50 μg ml^{-1} hygromycin. These cultures were plated onto Middlebrook 7H10 supplemented with 10% ADC, 2% sucrose, and 50 μg ml^{-1} hygromycin and incubated at 39°C for 3 weeks. The genomic incorporation of the plasmid was confirmed via the inability of colonies to grow on Middlebrook 7H10 supplemented with 25 μg ml^{-1} kanamycin.

The transformant used for experiments, termed Δ*ctpV*, was confirmed via negative PCR for the *ctpV* coding region and positive PCR for the hygromycin resistance cassette with primers listed in Table S3. Additionally, Southern blot was performed on Δ*ctpV* and wild-type genomic DNA (5 μg) digested with BamHI (Promega), using probes for the remaining coding region of *ctpV* or the hygromycin resistance cassette. For Southerns, the Promega Prime-A-Gene kit was used as directed by the manufacturer.

For complementation of Δ*ctpV*, the *ctpV* coding region was amplified and cloned into the pGEM-T easy vector for sequencing. The pGEM vector was then digested with EcoRI and HindIII (Promega), and the fragment was ligated into pMV361, which contains a kanamycin resistance cassette (Stover *et al*., 1991). The vector was sequenced, and then electroporated into electrocompetent Δ*ctpV* cells and plated on 7H10 supplemented with 10%ADC with 50 μg ml^{-1} hygromycin and 25 μg ml^{-1} kanamycin. The complemented strain was confirmed using a forward primer within the pMV361 vector (*hsp60*) and a reverse primer within the *ctpV* coding region.

M. smegmatis *strains and experiments*

To create *M. smegmatis*::*cso*, the *cso* operon from *Mtb* was amplified using Herculase Taq DNA polymerase (Stratagene, Santa Clara, CA, USA) and primers listed in Table S3. The fragment was digested with EcoRI (Promega) and cloned into plasmid pUC18. After verification of the fragment via sequencing, the plasmid was digested by EcoRI, blunt-ended with Klenow, and cloned into a pSE100 vector that had previously been double digested with EcoRI and HindIII and blunt-ended with Klenow. *M. smegmatis* mc^{2}155 was electroporated with an integrative vector containing *tetR* under an intermediate promoter, and selected for on 7H10 plates containing kanamycin. The pSE100::*cso* vector was electroporated into this recombinant *M. smegmatis* strain. For copper exposure experiments, *M. smegmatis*::*cso* or *M. smegmatis*

electroporated with an empty pSE100 vector were grown in 7H9 + ADC to OD 1.0, pelleted and washed twice in Sauton's, and then used to inoculate 50 ml cultures of Sauton's to OD 0.1, with ATC added to cultures of both strains to 40 ng ml^{-1}. These cultures were allowed to grow to OD 1.0 prior to addition of $CuCl_2$ to 5 mM. After 3 h of exposure, cultures were pelleted and washed twice in Sauton's, then dried at 100°C prior to submitting for NAA analysis.

Neutron activation analysis experiments

Mycobacterium smegmatis culture pellets were irradiated and analysed at the University of Wisconsin Nuclear Reactor (UWNR), a 1.0 MW TRIGA reactor. The detector was an Ortec High Purity Germanium detector (ORTEC, Oak Ridge, TN). Samples were irradiated with a thermal neutron flux of approximately 5E12 nv (neutrons per cm^2 per second). Irradiation time was 10.6 s. After 3 min decay time, each vial was counted for 300 s, and analysis was performed by the UWNR compiled program NAACalc version 1.41.

Growth experiments

Growth experiments in rich media used Middlebrook 7H9 liquid media (Remel, Lenexa, KS), prepared as described by the manufacturer and supplemented with 10% ADC and 0.05% Tween. Minimal media growth experiments were performed in Sauton's minimal media (which is free of copper) (Parish and Stoker, 1998), supplemented with 0.05% Tween, prepared using water treated with Chelex (Sigma-Aldrich, St Louis, MO, USA). Glassware was acid-washed (1N nitric acid) to maintain metal-free conditions. Cultures were seeded to OD_{600} 0.1 with bacterial stock washed 2 × in Sauton's, and allowed to grow for 14 days at 37°C with shaking. Colony-forming units were determined by plating on Middlebrook 7H10 + 10% ADC solid media, with 50 μg ml^{-1} hygromycin added in the case of the mutant and complemented strains.

Scanning electron microscopy

After growth to OD_{600} 0.6 in copper-free media, cultures of H37Rv, Δ*ctpV* or Δ*ctpV*::*ctpV* were exposed to 500 μM $CuCl_2$ for 3 h in a 24-well tissue culture plate containing 12 mm glass coverslips. Coverslips were processed for SEM imaging as previously described (Wu *et al*., 2009). Briefly, coverslips were rinsed with Hanks' Balanced Salt Solution (Lonza Walkersville, Walkersville, MD, USA) and incubated overnight in a solution of 4% paraformaldehyde and 2.5% gluteraldehyde. After sequential alcohol dehydration, coverslips were dried in a Samdri 780-A critical point dryer (Tousimis, Rockville, MD, USA) and splatter-coated with gold-palladium prior to imaging with a Hitachi S-570 scanning electron microscope. Bacillus size was measured using Image Pro Plus (Media Cybernetics, Bethesda, MD,USA) and at least two images from each condition were analysed.

Mouse infections

BALB/c mice (Harlan Laboratories, Indianapolis, IN, USA) were infected in a Glas-Col chamber (Glas-Col, LLC, Terra Haute, IN, USA) loaded with 10 ml of either H37Rv, Δ*ctpV* or Δ*ctpV*::*ctpV* bacteria at an OD_{600} of 0.30. Infectious dose of approximately 300 cfu per animal was confirmed via a 1 day time point. Colony-forming units were determined by homogenizing lung tissue in PBS buffer and plating on Middlebrook 7H10 + 10%ADC, followed by incubation at 37°C for 1 month. For the survival curve, animals were monitored daily by animal care staff not associated with the study. As specified in our animal protocol, mice were sacrificed after being identified by our animal care staff as morbidly ill, using criteria such as haunched posture, extreme weight loss, and slow or pained movements. Sections of lung, liver and spleen tissue were taken and incubated in formalin prior to sectioning and staining with haematoxylin and eosin (H&E) and acid-fast staining (AFS). Histopathology slides were examined and scored by a pathologist not associated with the study. For immunohistochemistry, the primary antibody, rabbit anti-interferon gamma (Invitrogen), was diluted 1:1000 in Van Gogh Yellow antibody diluent (Biocare Medical, Concord, CA, USA) and incubated for one hour. Negative control slides received only diluent in lieu of antibody. Primary antibody was detected using biotinylated goat anti-rabbit IgG secondary antibody (Biocare Medical) and Streptavidin-horseradish peroxidase (Biocare Medical). Staining was visualized with DAB+ (diaminobenzidine) (Dako, Glostrup, Denmark) and counterstained with CAT haematoxylin (Biocare Medical) mixed 1:1 with distilled water.

Guinea pig infections

Female Hartley guinea pigs (250–300 g, Charles River) were used for these studies. All guinea pigs were housed in a Biosafety Level-3 (BSL-3), pathogen-free animal facility and were fed water and chow *ad libitum*. The animals were maintained and all procedures performed according to protocols approved by the Institutional Animal Care and Use Committee at the Johns Hopkins University School of Medicine. Separate groups of guinea pigs were aerosol-infected with wild-type *M. tuberculosis* H37Rv, Δ*ctpV* or Δ*ctpV*::*ctpV* using a Madison aerosol exposure chamber (College of Engineering Shops, University of Wisconsin, Madison, WI, USA) calibrated to deliver 50–100 bacilli per animal lung. Four guinea pigs from each group were sacrificed on days 1, 21, 42 after aerosol infection.

At the designated time points, lungs from sacrificed animals were removed aseptically, weighed, and assessed for gross pathology. The lungs were then homogenized for cfu enumeration and processed for histological examination. Guinea pig lungs were homogenized in 10–15 ml PBS using a Kinematica Polytron Homogenizer with a 12 mm generator within a BSL-III Glovebox Cabinet (Germfree, Ormond Beach, FL, USA). Serial 10-fold dilutions of lung homogenates were plated on 7H11 selective agar (BBL) except for day 1 lung samples, which were plated neat, and plates were incubated at 37°C. The number of viable bacilli was enumerated after 4 weeks of incubation. At various time points after infection, lung samples were fixed in 10% PBS-buffered formalin, embedded in paraffin, and processed for histology. Sections were stained with H&E and Ziehl–Neelsen for microscopic evaluation.

Microarray analysis

Cultures of Δ*ctpV* were inoculated to OD_{600} 0.1 in Sauton's media and allowed to grow shaking at 37°C to OD_{600} 0.6. At this point, they were supplemented with 500 μM $CuCl_2$ and incubated for three more hours prior to spinning down the cultures and freezing immediately at –80°C. Microarray data were obtained as described previously (Ward *et al*., 2008). Briefly, RNA was extracted using a Trizol-based method (Invitrogen), and treated with DNase I (Ambion, Austin, TX) to remove contaminating DNA. cDNA was synthesized from 1 μg total RNA using an Invitrogen SuperScript ds-cDNA synthesis kit in the presence of 250 ng genome-directed primers (Talaat *et al*., 2002). cDNA clean up, Cy3 labelling, hybridizations and washing steps were performed using the NimbleGen gene expression analysis protocol (Roche Nimblegen, Madison, WI, USA). Microarray chips were purchased from NimbleGen Systems, and they contained 19 probes (60-mers) for each of the 3989 open reading frames identified in the genome of *Mtb* H37Rv (Camus *et al*., 2002), with five replicates of the genome printed on each slide (total of 95 probes/gene). Slides were scanned using an Axon GenePix 4000B scanner (Molecular Devices Corporation, Sunnyvale, CA), and fluorescence intensity levels normalized to 1000. Significantly changed genes between H37Rv and Δ*ctpV* were determined using the EBArrays package in R (http://www.bioconductor.org). A cut-off value of 0.50 for the probability of differential expression, determined using a lognormal-normal (LNN) model, was used to determine statistically differentially expressed genes (Kendziorski *et al*., 2003). Full data are deposited in accordance with MIAME standards at Array Express (http://www.ebi.ac.uk/microarray-as/ae) accession code E-MEXP-2773.

Quantitative, real-time PCR

qRT-PCR was performed using a SYBR green-based protocol. cDNA was synthesized from DNase-treated RNA, obtained as described above, using SuperScript III (Invitrogen) as directed by the manufacturer, in the presence of 250 ng mycobacterial genome-directed primers (Talaat *et al*., 2002). A 100 ng cDNA was used as template in a reaction with iTaq SYBR green Supermix with ROX passive dye (Bio-Rad) in the presence of gene-specific primers (Table S3) at a concentration of 200 nM. Cycle conditions were 50°C for 2 min, 95°C for 3 min, and 40 cycles of 95°C for 15 s and 60°C for 30 s. Reactions were performed in triplicate on an AB7300 machine (Applied Biosystems, Foster City, CA, USA) with fluorescence read at the 60°C step. Threshold cycle values were normalized to 16S rRNA levels.

Statistical analysis

The Student's *t*-test was used to determine whether data sets were significantly different, with a cut-off value of $P < 0.05$. The log rank test was used to determine whether survival of infected animals were significantly different, with a cut-off value of $P < 0.05$.

Acknowledgements

The authors thank Ralph Albrecht and Joseph Heintz for SEM analysis, and Thomas Pier and the University of Wisconsin TRIP lab for immunohistochemistry. We thank Kevin Austin and the University of Wisconsin Nuclear Reactor Laboratory for NAA analyses. We thank the TARGET Tuberculosis Animal Research and Gene Evaluation Taskforce at Johns Hopkins University, including Paul Converse, Petros Karakousis and Michael Pinn. We also thank Joseph Dillard, Sarah Marcus and Chia-wei Wu for reading the manuscript, as well as our anonymous reviewers for their helpful feedback throughout the submission process. This work was supported by grant NIH-R21AI081120 to A.M.T and by NIH training grant T32GM007215 to S.K.W.

References

Agarwal, K., Sharma, A., and Talukder, G. (1989) Effects of copper on mammalian cell components. *Chem Biol Interact* **69:** 1–16.

Avery, S., Howlett, N., and Radice, S. (1996) Copper toxicity towards *Saccharomyces cerevisiae*: dependence on plasma membrane fatty acid composition. *Appl Environ Microbiol* **62:** 3960–3966.

Bardarov, S., Bardarov, S.J., Jr, Pavelka, M.J., Jr, Sambandamurthy, V., Larsen, M., Tufariello, J., *et al*. (2002) Specialized transduction: an efficient method for generating marked and unmarked targeted gene disruptions in *Mycobacterium tuberculosis, M. bovis* BCG and *M. smegmatis*. *Microbiology* **148:** 3007–3017.

Beisel, W.R., Pekarek, R.S., and Wannemacher, R.W. (1974) The impact of infectious disease on trace-element metabolism of the host. In *Trace Element Metabolism in Animals-2*. Hoekstra, W.G., Suttie, J.W., Ganther, H.E., and Mertz, W. (eds). Baltimore, MD: University Park Press, p. 217.

Camus, J., Pryor, M., Médigue, C., and Cole, S. (2002) Re-annotation of the genome sequence of *Mycobacterium tuberculosis* H37Rv. *Microbiology* **148:** 2967–2973.

Casanova, J., and Abel, L. (2002) Genetic dissection of immunity to mycobacteria: the human model. *Annu Rev Immunol* **20:** 581–620.

Chung, J., Haile, D., and Wessling-Resnick, M. (2004) Copper-induced ferroportin-1 expression in J774 macrophages is associated with increased iron efflux. *Proc Natl Acad Sci USA* **101:** 2700–2705.

De Voss, J., Rutter, K., Schroeder, B., Su, H., Zhu, Y., and Barry, C.r. (2000) The salicylate-derived mycobactin siderophores of *Mycobacterium tuberculosis* are essential for growth in macrophages. *Proc Natl Acad Sci USA* **97:** 1252–1257.

Fleming, R., Whitman, I., and Gitlin, J. (1991) Induction of ceruloplasmin gene expression in rat lung during inflammation and hyperoxia. *Am J Physiol* **260:** L68–L74.

Flynn, J., and Chan, J. (2001) Immunology of tuberculosis. *Annu Rev Immunol* **19:** 93–129.

Francis, M., and Thomas, C. (1997) Mutants in the CtpA copper transporting P-type ATPase reduce virulence of *Listeria monocytogenes*. *Microb Pathog* **22:** 67–78.

Gold, B., Deng, H., Bryk, R., Vargas, D., Eliezer, D., Roberts, J., *et al*. (2008) Identification of a copper-binding metallothionein in pathogenic mycobacteria. *Nat Chem Biol* **4:** 609–616.

Graubner, W., Schierhorn, A., and Brüser, T. (2007) DnaK plays a pivotal role in Tat targeting of CueO and functions beside SlyD as a general Tat signal binding chaperone. *J Biol Chem* **282:** 7116–7124.

Kendziorski, C., Newton, M., Lan, H., and Gould, M. (2003) On parametric empirical Bayes methods for comparing multiple groups using replicated gene expression profiles. *Stat Med* **22:** 3899–3914.

Kershaw, C., Brown, N., Constantinidou, C., Patel, M., and Hobman, J. (2005) The expression profile of *Escherichia coli* K-12 in response to minimal, optimal and excess copper concentrations. *Microbiology* **151:** 1187–1198.

Liu, T., Ramesh, A., Ma, Z., Ward, S., Zhang, L., George, G., *et al*. (2007) CsoR is a novel *Mycobacterium tuberculosis* copper-sensing transcriptional regulator. *Nat Chem Biol* **3:** 60–68.

Lopez, A.D., Mathers, C.D., Ezzati, M., Jamison, D.T., and Murray, C.J.L. (2006) *Global Burden of Disease and Risk Factors*. New York: Oxford University Press, The World Bank.

Macomber, L., and Imlay, J. (2009) The iron-sulfur clusters of dehydratases are primary intracellular targets of copper toxicity. *Proc Natl Acad Sci USA* **106:** 8344–8349.

MacPherson, I., and Murphy, M. (2007) Type-2 copper-containing enzymes. *Cell Mol Life Sci* **64:** 2887–2899.

Marrichi, M., Camacho, L., Russell, D., and DeLisa, M. (2008) Genetic toggling of alkaline phosphatase folding reveals signal peptides for all major modes of transport across the inner membrane of bacteria. *J Biol Chem* **283:** 35223–35235.

Meharg, A.A. (1994) Integrated tolerance mechanisms: constitutive and adaptive plant responses to elevated metal concentrations in the environment. *Plant Cell Environ* **17:** 989–993.

Mitrakul, K., Loo, C., Hughes, C., and Ganeshkumar, N. (2004) Role of a *Streptococcus gordonii* copper-transport operon, *copYAZ*, in biofilm detachment. *Oral Microbiol Immunol* **19:** 395–402.

Ohsumi, Y., Kitamoto, K., and Anraku, Y. (1988) Changes induced in the permeability barrier of the yeast plasma membrane by cupric ion. *J Bacteriol* **170:** 2676–2682.

Parish, T., and Stoker, N.G. (1998) *Mycobacteria Protocols*. Totowa, NJ: Humana Press.

Pelicic, V., Jackson, M., Reyrat, J., Jacobs, W.J., Gicquel, B., and Guilhot, C. (1997) Efficient allelic exchange and transposon mutagenesis in *Mycobacterium tuberculosis*. *Proc Natl Acad Sci USA* **94:** 10955–10960.

Percival, S. (1998) Copper and immunity. *Am J Clin Nutr* **67:** 1064S–1068S.

Petrie, A., and Watson, P.F. (2006) *Statistics for Veterinary and Animal Science*. Oxford: Blackwell Pub.

Pinto, E., Sigaud-kutner, T.C.S., Leitao, M.A.S., Okamoto, O.K., Morse, D., and Colepicolo, P. (2003) Heavy-metal induced oxidative stress in algae. *J Phycol* **39:** 1008–1018.

Rook, G., Attiyah, R., and Filley, E. (1991) New insights into the immunopathology of tuberculosis. *Pathobiology* **59:** 148–152.

Schaible, U., and Kaufmann, S. (2004) Iron and microbial infection. *Nat Rev Microbiol* **2:** 946–953.

Schnappinger, D., Ehrt, S., Voskuil, M., Liu, Y., Mangan, J., Monahan, I., *et al*. (2003) Transcriptional adaptation of *Mycobacterium tuberculosis* within macrophages: insights into the phagosomal environment. *J Exp Med* **198:** 693–704.

Schwan, W., Warrener, P., Keunz, E., Stover, C., and Folger, K. (2005) Mutations in the *cueA* gene encoding a copper homeostasis P-type ATPase reduce the pathogenicity of *Pseudomonas aeruginosa* in mice. *Int J Med Microbiol* **295:** 237–242.

Smith, I. (2003) *Mycobacterium tuberculosis* pathogenesis and molecular determinants of virulence. *Clin Microbiol Rev* **16:** 463–496.

Stover, C., de la Cruz, V., Fuerst, T., Burlein, J., Benson, L., Bennett, L., *et al*. (1991) New use of BCG for recombinant vaccines. *Nature* **351:** 456–460.

Talaat, A., Howard, S., Hale, W., Lyons, R., Garner, H., and Johnston, S. (2002) Genomic DNA standards for gene expression profiling in *Mycobacterium tuberculosis*. *Nucleic Acids Res* **30:** e104.

Talaat, A., Lyons, R., Howard, S., and Johnston, S. (2004) The temporal expression profile of *Mycobacterium tuberculosis* infection in mice. *Proc Natl Acad Sci USA* **101:** 4602–4607.

Teitzel, G., Geddie, A., De Long, S., Kirisits, M., Whiteley, M., and Parsek, M. (2006) Survival and growth in the presence of elevated copper: transcriptional profiling of copper-stressed *Pseudomonas aeruginosa*. *J Bacteriol* **188:** 7242–7256.

Teixeira, E., Franco de Oliveira, J., Marques Novo, M., and Bertolini, M. (2008) The copper resistance operon *copAB* from *Xanthomonas axonopodis* pathovar citri: gene inactivation results in copper sensitivity. *Microbiology* **154:** 402–412.

Versieck, J. (1994) Neutron activation analysis for the determination of trace elements in biological materials. *Biol Trace Elem Res* **43–45:** 407–413.

Wagner, D., Maser, J., Lai, B., Cai, Z., Barry, C.r., Höner Zu Bentrup, K., *et al*. (2005) Elemental analysis of *Mycobacterium avium*-, *Mycobacterium tuberculosis*-, and *Mycobacterium smegmatis*-containing phagosomes indicates pathogen-induced microenvironments within the host cell's endosomal system. *J Immunol* **174:** 1491–1500.

Wang, Y., Hemmingsen, L., and Giedroc, D.P. (2005) Structural and functional characterization of *Mycobacterium tuberculosis* CmtR, a PbII/CdII-sensing SmtB/ArsR metalloregulatory repressor. *Biochemistry* **44:** 8976–8988.

Ward, S., Hoye, E., and Talaat, A. (2008) The global responses of *Mycobacterium tuberculosis* to physiological levels of copper. *J Bacteriol* **190:** 2939–2946.

White, C., Kambe, T., Fulcher, Y., Sachdev, S., Bush, A., Fritsche, K., *et al*. (2009) Copper transport into the secretory pathway is regulated by oxygen in macrophages. *J Cell Sci* **122:** 1315–1321.

Wu, C.W., Schmoller, S.K., Bannantine, J.P., Eckstein, T.M., Inamine, J.M., Livesey, M., *et al*. (2009) A novel cell wall lipopeptide is important for biofilm formation and pathogenicity of *Mycobacterium avium* subspecies paratuberculosis. *Microb Pathog* **46:** 222–230.

Zhang, X.-X., and Rainey, P.B. (2007) The Role of a P1-Type ATPase from *Pseudomonas fluorescens* SBW25 in Copper Homeostasis and Plant Colonization. *Mol Plant Microbe Interact* **20:** 581–588.

Supporting information

Additional supporting information may be found in the online version of this article.

Please note: Wiley-Blackwell are not responsible for the content or functionality of any supporting materials supplied by the authors. Any queries (other than missing material) should be directed to the corresponding author for the article.